J. Fluid Mech. (2003), *vol.* 474, *pp.* 117–145.
DOI: 10.1017/S0022112002002604 Printed in the United Kingdom

The flow field and bare-spot formation in spin-up from rest of a two-layer fluid about a vertical axis

By M. UNGARISH[1] AND J. MANG[2]

[1]Department of Computer Science, Technion, Haifa 32000, Israel

[2]Institute of Fluid Mechanics, Graz University of Technology, Graz, Austria

(Received 14 January 2002 and in revised form 24 April 2002)

The spin-up from rest of a two-layer fluid with a free surface in a cylindrical container rotating about a vertical axis is investigated for small Ekman numbers. Numerical results from the axisymmetric Navier–Stokes equations, supported by comparisons with improved boundary-layer approximations, show that the Ekman-type layer on the bottom pushes the dense fluid of the lower layer to the periphery, and consequently the interface between the layers curves upward near the sidewall and descends near the centre. When the lower layer of fluid is sufficiently thin a bare spot appears at the bottom, i.e. a region where the light fluid is in direct contact with the horizontal boundary. The lower-layer fluid is spun-up quickly by the bottom Ekman layer, but the angular motion in the upper layer is provided by the much weaker detached Ekman layer on the interface between the two fluids, and hence the global spin-up process is prolonged compared with the homogeneous fluid case. The influence of the various dimensionless parameters and the connection with the continuous stratified case are discussed.

1. Introduction

The spin-up from rest of a pure fluid in a cylindrical container of radius R^*, instantaneously set into rapid rotation with the angular velocity Ω^* about its vertical axis of symmetry z, is a fundamental problem in rotating flows. It represents an essential stage in the operation of centrifuges and is of great relevance in the investigation of geophysical flows. In the configurations of interest the value of the Ekman number, $E = \nu^*/(\Omega^* R^{*2})$, is very small, where ν^* is the kinematic viscosity of the fluid.

The classical linear theory of Greenspan & Howard (1963) describes the differential spin-up of a homogeneous fluid in a closed container after a small increase $\Delta\Omega$ of its angular velocity. Goller & Ranov (1968) considered the flow in a cylinder with a free surface. Wedemeyer (1964) developed an analytical model for the spin-up from rest which concerns the transient process during which the initially stationary fluid acquires a state of solid-body rotation with the angular velocity of the container. In both the linear and nonlinear cases, the main transient flow field in the core is driven by a secondary $O(E^{1/2})$ convective motion, induced by the 'suction' or 'pumping' of the quasi-steady thin viscous Ekman layer on the horizontal solid boundary (or boundaries, if the container is closed). The remarkable feature is that the Ekman-layer suction activates the fluid in the entire core, so that the angular acceleration of the fluid is almost completed on the spin-up timescale, which is significantly shorter than the viscous diffusion time interval.

The fascinating spin-up phenomenon has numerous ramifications, as indicated by the recent review by Duck & Foster (2001). An interesting aspect, from both academic

and practical viewpoints, is the effect of stratification on the spin-up process. Let the gravitational acceleration be in the $-z$-direction. The presence of a density gradient or density jump introduces an axial buoyancy force which imposes a limitation on the axial distance from the bottom accessed by the Ekman pumping effect. For spin-up from rest this means that there may be large fluid domains which cannot be spun-up by being flushed through the Ekman layer on the solid boundary. In particular, the spin-up of two-layer liquid systems has received some consideration in the past. Determination of exact spin-up times is important for the design of centrifuges used in chemical and biological engineering applications. The transient shape of the interface between the fluids must be known for the positioning of fluid intakes and discharges (Berman, Bradford & Lundgren 1978; Lim, Choi & Hyun 1993). Other applications are in geophysical flows of oceans and the atmosphere (Pedlosky 1967; Linden & van Heijst 1984). The spin-up of two-layer liquid systems is also of particular relevance to the investigation of rotating gravity currents with a lock release of the heavy fluid when it is necessary to create a specific initial state (Hallworth, Huppert & Ungarish 2001).

Linden & van Heijst (1984) performed an experimental investigation of the differential spin-up about a vertical axis of a two-layer system with a thin lower layer and a free surface. An important feature of the system investigated was the formation of a bare spot which occurs when the transient interface (between the upper and lower fluids) intersects the bottom of the container. The term 'bare spot' refers to the area in which the upper-layer fluid contacts the bottom plate. The formation of bare spots is relevant to oceanographic flows because it provides a mechanism for the removal of sediments into fluid layers which are typically not in contact with the sea bottom (Lambert *et al.* 1983). Linden & van Heijst also developed a theory for the prediction of the radius and formation time of a stationary bare spot. This theory, however, is based on severe simplifying assumptions such as the neglect of viscous coupling at the interface and the assumption of a completely spun-up lower layer. In the spin-up from rest case, not considered by Linden & van Heijst (1984), the Ekman layers play a more dramatic role than in the differential spin-up case because no angular momentum is present in the container at the beginning, and large domains of zero absolute vorticity persist during the spin-up process. The spin-up from rest mechanism requires the flushing of all the fluid particles through the Ekman layers, as opposed to the differential (in particular linear) case where inviscid displacement-stretching of fluid particles may produce local spin-up.

The spin-up from rest of a two-layer fluid system was considered by Lim *et al.* (1993) by means of both experiments in a closed container and an approximate analytical model. The analysis focused on systems in which both layers are of comparable thickness, and concentrated on the effect of large differences in kinematic viscosities between the fluids. It deliberately excluded the cases in which the interface intersects the horizontal boundary of the container, i.e. the bare spot phenomenon. In a sequel paper Kim & Hyun (1994) presented a numerical solution of the aforementioned problem, capturing the deforming interface by a volume-of-fluid method.

The present work attempts to enhance knowledge about the transient process leading to the formation of a bare spot in spin-up from rest, by means of a numerical finite-difference solution of the axisymmetric Navier–Stokes equations supported by an approximate boundary-layer model. This investigation can be considered an extension of the studies of Kim & Hyun (1994) and Linden & van Heijst (1984). The main novel aspects in our work are: (*a*) the development of the bare spot in spin-up from rest, with emphasis on configurations with a free upper boundary, a thin lower

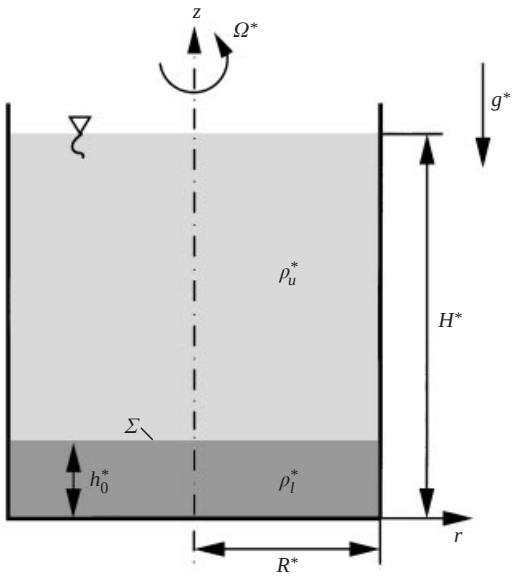

FIGURE 1. Sketch of the system at the start of the spin-up process, $t^* = 0$.

layer and thick upper layer, for fluids with (slightly) different densities but similar viscosities; (*b*) the behaviour of the total angular momentum in the container, and (*c*) the incorporation of new ingredients which have not been used in the previous investigations in the numerical results and the approximate model (e.g. the Ekman layer on the interface, an analytical result for the spin-up of the lower core), which are expected to improve the analysis.

The structure of the paper is as follows. A brief description of the problem is presented in § 2. The Navier–Stokes formulation and numerical method of solution are presented in § 3. Typical numerical results are displayed and discussed in § 4; in this context, an asymptotic (for small E) boundary-layer model is also introduced and compared. Some concluding remarks are given in § 5.

2. Description of the problem

The spin-up from rest of a two-layer stratified fluid is considered. An initially stationary cylindrical container of radius R^* and height H^*, open to the atmosphere, is filled with two fluids (e.g. fresh and salt water) of (slightly) different densities ρ_u^* and ρ_l^*, with $\rho_l^* > \rho_u^*$, but equal dynamic viscosities (figure 1). The subscripts u and l denote the upper and the lower fluid, respectively. Dimensional variables are marked by an asterisk. The interface between the fluids, denoted Σ, is initially horizontal and at height h_0^* above the bottom. At the time $t^* = 0^+$ the container is abruptly set into rapid rotation about its vertical axis with the constant angular velocity Ω^*. The objective is the description of the flow field and the understanding of the mechanisms and timescales which govern the motion. The behaviour of the height of the interface $h^*(r^*, t^*)$ is of particular interest. We assume that $\Omega^{*2} R^*/g^* \ll 1$ and hence the deformation of the upper free surface during and after the spin-up process is negligible.

The essential global feature is, evidently, the increase of the total angular momentum of the fluid in the container. In a rotating cylindrical coordinate system this property

can be expressed as (per radian)

$$\Gamma(t) = \int_0^H \int_0^1 \rho[\omega(r,z,t)+1]r^3 \,\mathrm{d}r\,\mathrm{d}z, \tag{2.1}$$

where the lengths are scaled by R^*, the angular velocity ω by Ω^*, time by Ω^{*-1} and the density by ρ_u^*. For simplicity assume here $\rho = 1$. Initially $\Gamma = 0$ and at the fully spun-up state $\Gamma(\infty) = 0.25H$. The increase of Γ is provided by the friction on the boundaries. The viscous layer on the sidewall thickens with time to $O(E^{1/4})$, but the Ekman-like layer on the bottom, which reduces the angular velocity from $\omega(z = 0^+, r, t) < 0$ in the fluid core above the bottom to the zero boundary condition, maintains a constant thickness $O(E^{1/2})$ (after an initial period of formation of about one revolution). We therefore expect that the azimuthal shear stress at the bottom is, roughly, $E^{-1/2}\omega(z = 0^+, r, t)r$, and dominant $(\mu^*\partial(\omega^* r^*)/\partial z^*$ is scaled with $\rho_u^*\Omega^{*2}R^{*2})$. The torque M of this Ekman layer is the governing contributor to angular momentum increase, i.e.

$$\frac{\mathrm{d}\Gamma}{\mathrm{d}t} \approx M = -E\int_0^1 \left(\frac{\partial\omega}{\partial z}\right)_{z=0} r^3\,\mathrm{d}r \approx -E^{1/2}\int_0^1 \omega(z=0^+,r,t)r^3\,\mathrm{d}r. \tag{2.2}$$

Evidently, the most effective torque is $M_0 = 0.25E^{1/2}$, applied at the beginning, when the angular velocity in the core adjacent to the Ekman layer (position denoted by $z = 0^+$) is -1. Under the corresponding maximal constant torque the value of $\Gamma(\infty)$ could be attained at $t \approx HE^{-1/2}$, but this is certainly an underestimate of the spin-up time, because the fluid above the Ekman layer is spun-up during the process (i.e. $\omega(z = 0^+)$ is reduced) and the torque of the bottom decays. The important question is what portion of the inner fluid is spun-up before the Ekman layer torque M decays to, say, e^{-2} of its initial value M_0. Afterwards, the spin-up (if still necessary) can be caused only by the diffusion mechanism on the $O(E^{-1})$ timescale. To answer that question we must know where the partly spun-up fluid accumulates. In a homogeneous fluid system the partly spun-up fluid concentrates in an annulus adjacent to the outer wall (Wedemeyer 1964; Weidman 1976*a*, *b*; Hyun *et al.* 1983), see below. On the other hand, in a two-layer stratified system the vertical motion of fluid particles is hindered by gravity-buoyancy effects. In this case the partly spun-up fluid tends to concentrate near the bottom and therefore enhances the decay of the Ekman-layer torque; the result is, as shown in this paper, in particular in § 4, a more complex and significantly longer spin-up process than in the classical homogeneous case.

It is worthwhile to briefly recall some details of that classical flow, see figure 2. Within the first revolution, at the horizontal bottom of the container a quasi-steady viscous Ekman-type layer (of thickness $O(E^{1/2})$, region II) appears. The flow in the core above the Ekman layer remains essentially inviscid, with z-independent radial and angular velocities. The Ekman layer constantly sucks fluid from the non-rotating inner core (region I). Inside the Ekman layer, the fluid acquires angular velocity due to viscous friction from the boundary. This fluid is pumped from the centre to the periphery and finally expelled into the partly spun-up region III. Thereby, a secondary convective core flow is created. Regions I and III are separated by an inwardly moving cylindrical spin-up front. The approximation presented by Wedemeyer (1964), indicates that for $E \to 0$ the spin-up is performed by the Ekman layers, and yields a simple analytical solution for the flow field in the interior, see Appendix A. This

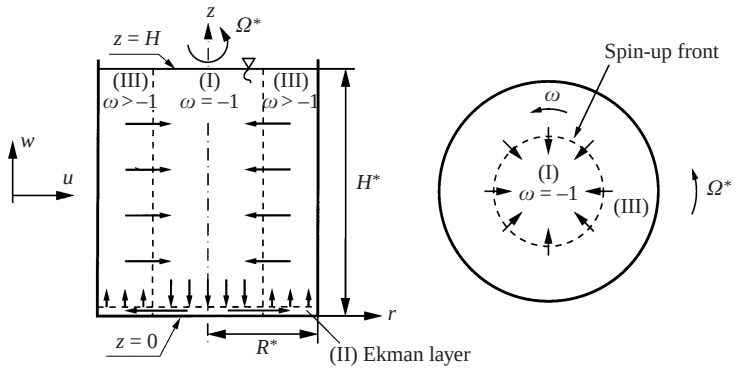

FIGURE 2. Flow regions in spin-up from rest of a homogeneous fluid (side and top views in a rotating system).

predicts that the radial position of the front is $\exp(-\tau)$ and

$$\frac{\Gamma(t)}{\Gamma(\infty)} = 1 - \mathrm{e}^{-2\tau}, \tag{2.3}$$

where τ is the time scaled with

$$\tau^*_{su} = 2H/(E^{1/2}\Omega^*). \tag{2.4}$$

In the present configuration, the density of the fluid expelled by the Ekman layer is larger than that of the fluid in the upper layer. Consequently, the spun-up particles of fluid expelled axially near the outer wall can travel upward easily while embedded in the dense fluid, but are strongly hindered after they reach the height of the interface. In other words, the density jump at the interface prevents the spun-up fluid from the Ekman layer from entering the region of light upper fluid. Thus, the thin lower layer acts as a buffer between the bottom Ekman layer and the upper fluid, and hence the spin-up of the two-fluid system is significantly delayed compared to the one-fluid configuration. The interface will descend in the region where the Ekman layer sucks fluid in and rise where it expels fluid. If the lower layer is thin and the stratification is weak, the central part of the interface may even come into contact with the bottom wall and form a bare spot. However, when both fluids eventually acquire the angular velocity of the container, the interface must attain the shape of the classical equilibrium parabola (see Appendix C, (C 2) and (C 3)):

$$h^* = h^*_0 - \frac{\Omega^{*2}R^{*2}}{4g^*}\left[1 - 2\left(\frac{r^*}{R^*}\right)^2\right]. \tag{2.5}$$

It is convenient to start the more detailed investigation of the two-fluid problem by means of numerical experiments performed with a numerical solution of the axisymmetric Navier–Stokes equations. The transient flow field before and early after the formation of a bare spot is focused on.

3. Numerical simulation

3.1. *Formulation*

The governing equations are formulated in a cylindrical coordinate system rotating with angular velocity Ω^* about the vertical axis z. The gravitational acceleration is $-g^*\hat{\boldsymbol{z}}$. The velocity vector is denoted by $\boldsymbol{v} = u\hat{\boldsymbol{r}} + v\hat{\boldsymbol{\theta}} + w\hat{\boldsymbol{z}}$ in terms of the unit vectors $\hat{\boldsymbol{r}}, \hat{\boldsymbol{\theta}}, \hat{\boldsymbol{z}}$ in the radial, azimuthal and axial directions.

The density of the lower-layer fluid is ρ_l^* and that of the upper-layer fluid ρ_u^*. It is convenient to describe the density field by means of a density function, $\phi(\boldsymbol{r}, t)$, which is defined by

$$\rho^*(\boldsymbol{r}, t) = \rho_u^*[1 + \epsilon\phi(\boldsymbol{r}, t)], \tag{3.1}$$

where

$$\epsilon = (\rho_l^* - \rho_u^*)/\rho_u^*. \tag{3.2}$$

Hence, it is expected that $0 \leqslant \phi \leqslant 1$, with $\phi = 1$ in the 'pure' dense-fluid domain and $\phi = 0$ in the 'pure' upper-fluid domain. The moving interface $\Sigma(\boldsymbol{r}, t)$ is captured by solving a transport equation for ϕ.

The analysis is conveniently performed with dimensionless variables obtained by using the scaling

$$[\boldsymbol{r}^*, \boldsymbol{v}^*, t^*, P^*] = [R^*\boldsymbol{r}, R^*\Omega^*\boldsymbol{v}, \Omega^{*^{-1}}t, \rho_u^*(\Omega^*R^*)^2P]. \tag{3.3}$$

The governing equations are:

(i) continuity of volume

$$\nabla \cdot \boldsymbol{v} = 0; \tag{3.4}$$

(ii) momentum balance

$$\frac{\mathrm{D}\boldsymbol{v}}{\mathrm{D}t} + 2\hat{\boldsymbol{z}} \times \boldsymbol{v} = \frac{1}{1 + \epsilon\phi}[-\nabla p + \phi\boldsymbol{f} + E\nabla^2\boldsymbol{v}], \tag{3.5}$$

with the reduced pressure

$$p = P - \left(\frac{r^2}{2} - \frac{g^*}{\Omega^{*2}R^*}z\right), \tag{3.6}$$

and the body-force acceleration $\boldsymbol{f}$ given by

$$\boldsymbol{f} = \epsilon r\hat{\boldsymbol{r}} - \frac{1}{Fr^2}\hat{\boldsymbol{z}}; \tag{3.7}$$

(iii) dense fluid transport

$$\frac{\mathrm{D}\phi}{\mathrm{D}t} = \nabla \cdot \mathscr{D}\nabla\phi. \tag{3.8}$$

The relevant dimensionless parameters, in addition to ϵ defined above, are the Ekman number

$$E = \frac{\mu^*}{\rho_u^*\Omega^*R^{*^2}}, \tag{3.9}$$

and the global Froude number (squared)

$$Fr^2 = \frac{\Omega^{*^2}R^*}{g'^*}, \quad \text{where} \quad g'^* = \epsilon g^*. \tag{3.10}$$

E represents the ratio of viscous to Coriolis effects in the global motion. Fr^2 is the ratio of the representative centrifugal and reduced gravity components of the body force. We assume the same viscosity μ^* for both fluids, but this can be easily relaxed. In the present scaling the Rossby number equals unity, which reflects the nonlinearity of the spin-up flow. The dimensionless geometric parameters of the configuration are the height of the container, H, and the initial thickness of the lower layer of fluid, h_0, both of the order of unity.

The present investigation focuses on flows with small values of E and ϵ and values

of Fr^2 of order unity. The diffusion coefficient $\mathscr{D}$ (the inverse of a Péclet number) is assumed very small even compared with E. (The typical physical value of $\mathscr{D}$ for a system of, say, salt-water layers, which is typical of our investigation, is negligibly small for the time periods considered, but here a non-zero $\mathscr{D}$ is used as an artificial diffusion coefficient for numerical smoothing of the large density gradients at the interface, otherwise some spurious numerical oscillations may appear.)

The initial conditions at $t = 0$ are

$$\boldsymbol{v} = -r\hat{\boldsymbol{\theta}} \;\forall\; 0 \leqslant r \leqslant 1, \quad 0 \leqslant z \leqslant H, \tag{3.11}$$

$$\phi = \begin{cases} 1 & \forall\; 0 \leqslant r \leqslant 1, \quad 0 \leqslant z \leqslant h_0, \\ 0 & \text{elsewhere.} \end{cases} \tag{3.12}$$

The boundary conditions for $t \geqslant 0^+$ are

$$\boldsymbol{v} = \boldsymbol{0} \quad \text{on the bottom and sidewalls,} \tag{3.13}$$

$$\boldsymbol{v} \cdot \hat{\boldsymbol{z}} = 0, \quad \text{no tangential stress at } z = H, \tag{3.14}$$

$$\text{regularity at the axis } r = 0, \tag{3.15}$$

and

$$\hat{\boldsymbol{n}} \cdot \nabla\phi = 0 \quad \text{on all boundaries.} \tag{3.16}$$

These conditions neglect the deformation of the free surface caused by the centrifugal and Coriolis effects. This simplification is convenient from the computational point of view, and is well-justified for the small values of $\Omega^{*2}R^*/g^*$ assumed here. To be more specific, it can be argued that the displacement of the interface during the spin-up process is smooth in time and its magnitude at the end of the process is bounded by $\Omega^{*2}R^{*2}/4g^*$. Note that $\Omega^{*2}R^*/g^*$ can be rewritten as ϵFr^2, and hence the assumption that the upper boundary is a frictionless solid lid introduces relative errors of magnitude $\epsilon Fr^2/4$ at most.

A Stokesian stream function $\psi(r, z, t)$ is defined by

$$u = \frac{1}{r}\frac{\partial\psi}{\partial z}, \quad w = -\frac{1}{r}\frac{\partial\psi}{\partial r}. \tag{3.17}$$

The angular velocity $\omega(r, z, t)$ in the rotating frame is given by

$$\omega = \frac{v}{r}. \tag{3.18}$$

The incorporation of the density transport equation (3.8) makes our formulation different from that used by Kim & Hyun (1994). Consequently, the latter needed a special numerical technique for tracking the interface, while in our solution the interface is simply captured by the sharp gradients of the function ϕ.

3.2. *Computations*

The foregoing system of equations and boundary conditions, subject to the axial-symmetry assumption, is solved by a time-marching finite difference discretization method.

Briefly, the method is based on forward-time formulation of the velocity components, with implicit Coriolis and pressure terms. At each time step, the continuity equation for the 'new' velocity field yields an elliptic equation for the 'new' pressure field, $p^+(r, z)$. The details are described in Appendix B. The numerical, staggered grid is sketched in figure 3. The discretized variables p and ϕ are defined at mid-cell

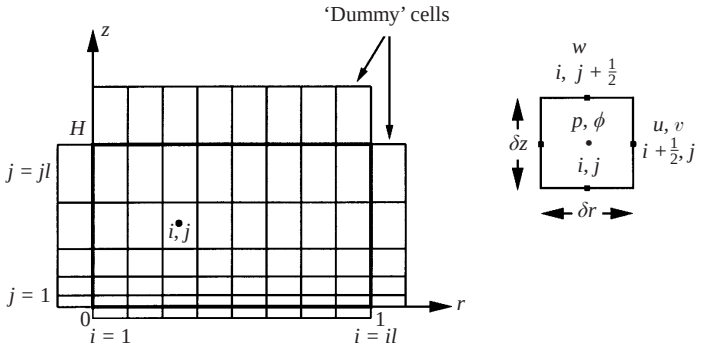

FIGURE 3. Spatial staggered grid, for $0 \leqslant r \leqslant 1$, $0 \leqslant z \leqslant H$, plus dummy boundary cells.

position, denoted (i, j); u and v are defined at the positions $(i \pm \frac{1}{2}, j)$ and w is defined at $(i, j \pm \frac{1}{2})$, for $i = 1(1)il$, and $j = 1(1)jl$ (in addition, dummy points are used to implement boundary conditions).

Both the r and z grid coordinates are stretched by simple mapping functions $r(\mathscr{R})$ and $z(\mathscr{Z})$. The grids $\mathscr{R}_i = (i - \frac{1}{2})\delta\mathscr{R}$ and $\mathscr{Z}_j = (j - \frac{1}{2})\delta\mathscr{Z}$ are uniform,

$$0 \leqslant \mathscr{R} \leqslant 1, \quad 0 \leqslant \mathscr{Z} \leqslant H, \tag{3.19}$$

$$\delta\mathscr{R} = 1/il, \quad \delta\mathscr{Z} = H/jl. \tag{3.20}$$

An illustration of the finite difference approach is

$$\left(\frac{1}{r}\frac{\partial}{\partial r} r \frac{1}{1+\epsilon\phi}\frac{\partial p}{\partial r}\right)_{r_i, z_j} \approx \frac{1}{r_i}\frac{1}{r_i'\delta\mathscr{R}}(Y_{i+1/2,j} - Y_{i-1/2,j}), \tag{3.21}$$

where

$$Y_{i+1/2,j} = r_{i+1/2}\frac{1}{1+\epsilon\phi_{i+1/2,j}}\frac{1}{r'_{i+1/2}\delta\mathscr{R}}(p_{i+1,j} - p_{i,j}), \tag{3.22}$$

and r_i' is the derivative of $r(\mathscr{R})$ at $\mathscr{R}_i$ (substituting $i - 1$ in place of i yields $Y_{i-1/2,j}$). The truncation error is $O(\delta\mathscr{R}^2 + \delta\mathscr{Z}^2)$.

The combination of the foregoing time and space discretizations is the core of the computer code used in this work. For each time step the discretized form of the Poisson equation (B 4) for the discretized variables $p^+_{i,j}$, with $1 \leqslant i \leqslant il$ and $1 \leqslant j \leqslant jl$, must be solved. This yields a block tri-diagonal linear system. The linear system was solved by a bi-conjugate gradient iterative algorithm (Press *et al.* 1992). The iterations in the first time step start with 0, and subsequently the p_{ij} field provides the starting values for p^+_{ij}. Some test cases were also run with a direct solver for the block tri-diagonal system. The computations use real-8 variables. The typical grid has $il = 100$ constant radial intervals and $jl = 200$ stretched axial intervals (this provides about seven axial intervals in the Ekman layer domain of thickness $3E^{1/2}$ considered in this work, see below). Verification runs were also performed on 100×150 and 120×200 grids. The agreement between the results on the different grids was excellent. The typical time step was $\delta t = 10^{-3}$. In several test cases δt was halved, without causing any significant differences in the results or stability. The diffusion coefficient $\mathscr{D}$ was defined as E/Sc, with Sc the Schmidt number. Sc was given the artificial value 10 in order to dampen non-physical numerical oscillations around the interface between the two fluids. The code was run on one processor on the following computers: SUN Ultra-Enterprise E4500 with 400 Mhz processors, and SG Origin with R10000/3.4

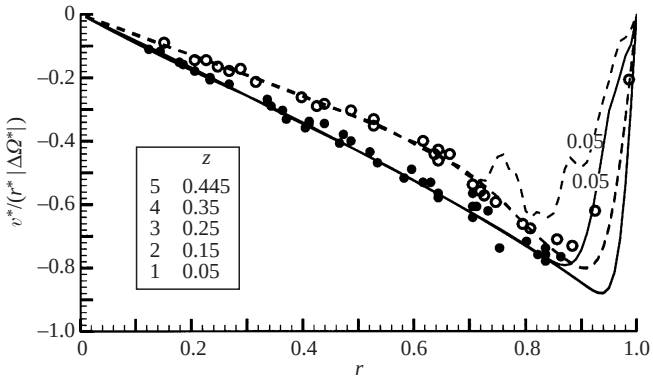

FIGURE 4. Present numerical results and experimental results by Linden & van Heijst (1984, figure 7*b*), for the free-surface azimuthal velocity $v(r)$ at $t = 4$ rev (solid curves and circles) and $t = 11$ rev (dashed curves and open circles): $\Delta\Omega/\Omega = -0.292$, $\epsilon = 1.02 \times 10^{-2}$, $Fr^2 = 0.89$, $E = 1.1 \times 10^{-5}$, $H = 0.45$, $h_0 = 2.01 \times 10^{-2}$. Note that profiles 2–5 collapse onto one line.

250 Mhz processors. Typical run times for the computation of the flow field presented below in one revolution physical time period were approximately 2.5 CPU hours for a 100×150 grid, and 6 CPU hours for a 100×200 grid.

Various test problems were used for the verification of the numerical code. In particular, for the spin-up from rest of a pure fluid in a closed cylindrical container of height $2H^*$, our results were in excellent agreement with the numerical results of Hyun *et al.* (1983). The present numerical code was also tested by comparison with the experimental data of Linden & van Heijst (1984) for the differential spin-up of a two-layer fluid in an open container. Figure 4 shows a comparison between experimental results (dots and circles) for $v(r)$ at the free surface (taken from figure 7(*b*) of the aforementioned paper) and the corresponding numerical results of our code at $t = 4$ rev (solid line) and $t = 11$ rev (dashed line). The frame of reference rotates with the final angular velocity. The numerical results correspond to five representative vertical positions inside the upper layer. The agreement between the numerical results and the experimental data is judged to be very good, within the range of the plausible experimental errors. The overlapping of the numerical results indicates that the angular velocity in the upper-layer domain is z-independent. The curves corresponding to $z = 0.05$ intersect the lower layer, which has already acquired a larger angular velocity.

4. Results

We present in some detail results for the following typical configuration: the height of the container is $H = 1$, the initial thickness of the lower fluid domain is $h_0 = 0.2$ and the Ekman number is $E = 5 \times 10^{-5}$. To achieve different values of Fr^2 we vary the density difference ϵ to produce different values of reduced gravity, see (3.10); this connects the present numerical experiments with feasible tests in which the geometry, angular velocity and density of the upper fluid (say water) are fixed, and the density of the lower layer is changed by addition of salt. To be more specific, a cylinder of radius $R^* = 10$ cm rotating with $\Omega^* = 2\,\mathrm{s}^{-1}$ and an upper layer of fresh water ($\nu^* = 0.01\,\mathrm{cm}^2\,\mathrm{s}^{-1}$) yields the basic physical setup for the results discussed below. The Froude numbers considered are achieved for the practical values of $g'^* = 5$ and $20\,\mathrm{cm\,s}^{-2}$. The dimensionless thickness of the Ekman-type layer at the bottom is

$\delta \approx 3\sqrt{E} = 0.021$. In a typical grid with 150 vertical intervals, there were about five mesh points within this axial span. Thus, a good resolution of this shear layer is anticipated (the accuracy of the volume flux is estimated as about 1%). The free Ekman layer which appears on the interface, as explained below, is thicker and smoother than the bottom layer, and hence good numerical resolution in this region is also found.

The spin-up interval for a homogeneous fluid in a similar configuration, $2HE^{-1/2}/\Omega^*$, is about 45 revolutions.

4.1. *Case* $\epsilon = 5.1 \times 10^{-3}$, $Fr^2 = 8$

In this case $g'^* = 5\,\mathrm{cm\,s^{-2}}$. Figure 5 shows contour plots of the density-function ϕ-field for successive times t. The grey corresponds to $\phi = 0$, i.e. pure upper-layer fluid and the black to $\phi = 1$, i.e. pure lower-layer fluid. The density jump at the interface is slightly smeared by numerical effects. We use a fixed-grid shock-capturing type approach to detect the position of the interface, and hence the moving discontinuities of density are smoothed over 2–3 grid intervals. Figures 6 and 7 show contour plots of ω and ψ.

Within the first revolution a quasi-steady thin Ekman layer develops at the bottom of the container. The Ekman layer transports fluid from the centre to the periphery. The Ekman layer below the non-rotating region sucks fluid in from the core and thereby causes the interface to descend. The Ekman layer below the partially spun-up region expels fluid into the core. However, a particle of the expelled fluid, of density $1 + \epsilon$, is subjected to a strong negative buoyant force when it attempts to move above the interface, and therefore the axial propagation of these particles is restricted. The interface moves up to accommodate the fluid expelled by the bottom Ekman layer, but this spun-up fluid is recirculated back to the centre before it reaches axial positions significantly larger than h_0.

Figure 6 shows the angular velocity field (in the rotating frame) $\omega(r, z)$ at two times. The (partly) spun-up fluid domain is near the periphery and in the bottom Ekman layer, and there is a clear non-rotating domain elsewhere. These domains are separated by a quite sharp spin-up front, which, for practical purposes, can be defined as the position of the contour $\omega = -0.95$, outside the Ekman layers. The spin-up front propagates radially inward and its upper part is vertical (like in the homogeneous fluid case), but its lower part is inclined. The spun-up domain contains two cores, each of essentially z-independent ω. It is evident that, at a fixed time, the spin-up process in the lower core is significantly more advanced that in the upper core. The cores with different ω are connected by an inclined layer of strong shear.

We emphasize that the spin-up observed in the upper layer of fluid, although slower than in the lower layer, is still much faster than that provided by the viscous diffusion of momentum from the sidewall. An estimate (based on Stokes first problem) shows that this diffusion produces

$$\omega = -\mathrm{erf}[0.5(1 - r)/(Et)^{1/2}] \tag{4.1}$$

and hence is able to establish the value $\omega = -0.95$ at the radial distance from the sidewall $\Delta = 0.049\sqrt{n}$ in the present problem, where n is the number of revolutions. This yields $\Delta = 0.099$ and 0.16 for $n = 4$ and 10, respectively. Figure 6 shows a much deeper penetration of the spin-up front in the upper layer of fluid. The conclusion is that the fluid in the upper layer is also subject to convective spin-up by Ekman layer action, in this case due to the shear at the interface between the fluids.

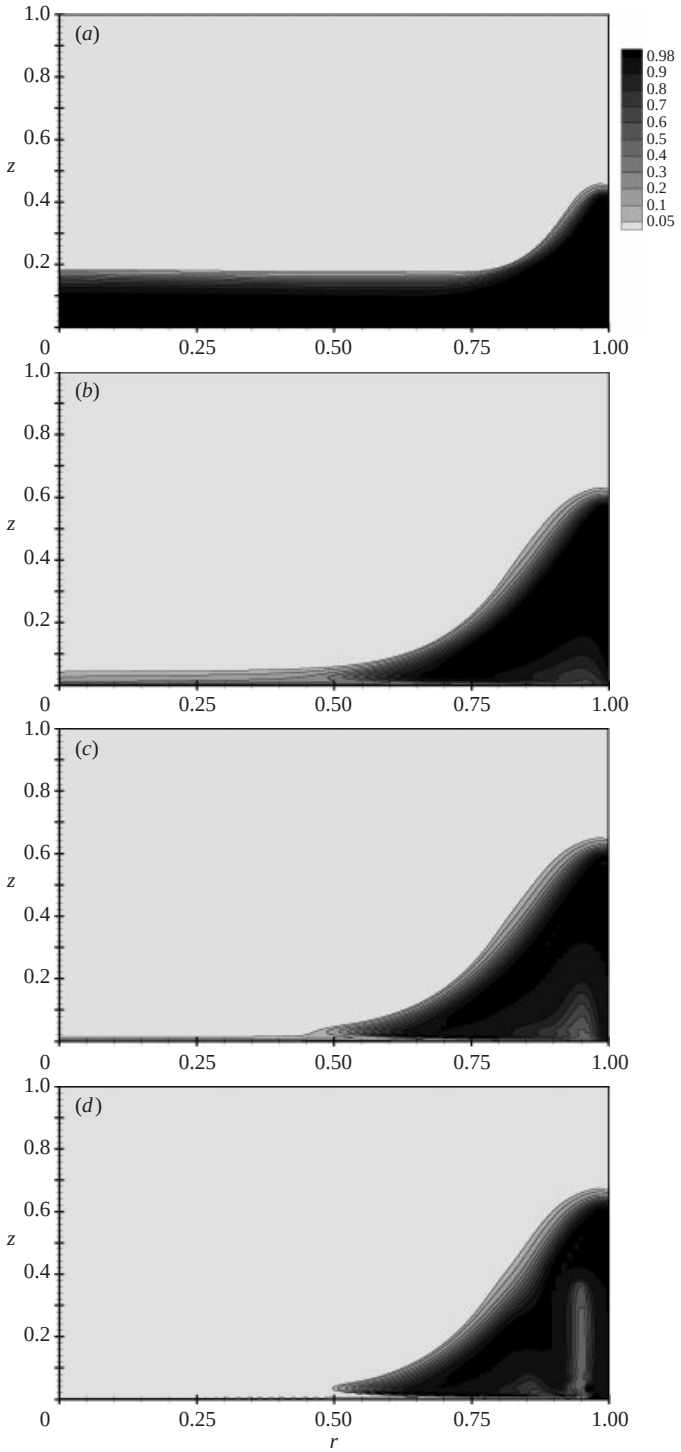

FIGURE 5. Density function $\phi(r, z)$ contour plots at successive t: (*a*) 4 rev, (*b*) 10 rev, (*c*) 11 rev, (*d*) 12 rev; $\epsilon = 5.1 \times 10^{-3}$, $Fr^2 = 8$, $E = 5 \times 10^{-5}$, $H = 1$, $h_0 = 0.2$.

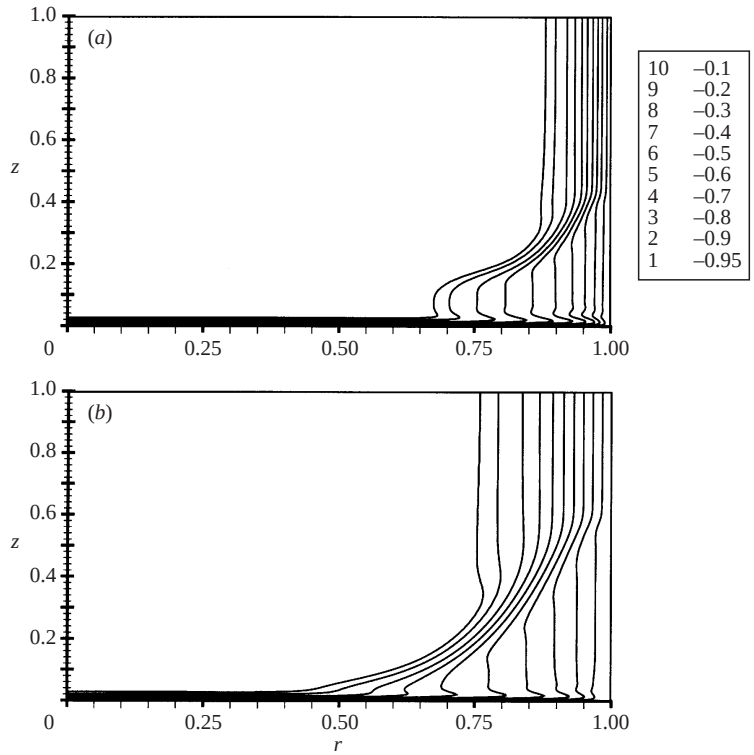

FIGURE 6. Angular velocity $\omega(r, z)$ contour lines at successive t: (*a*) 4 rev, (*b*) 10 rev; $\epsilon = 5.1 \times 10^{-3}$, $Fr^2 = 8$, $E = 5 \times 10^{-5}$, $H = 1$, $h_0 = 0.2$. The values of ω range from 0 at the solid wall to -1.00 in the non-rotating core.

It is seen in figure 5 that the interface consists of a horizontal and an inclined part. A comparison with figure 6 shows that the interface is horizontal in the region where the fluid in both layers is still non-rotating. The inclined part of the interface corresponds to the region where the lower layer is already partly spun-up.

The lower-layer fluid acts as a buffer between the bottom Ekman layer, which drives the flow, and the upper fluid. Therefore, the spin-up progresses much faster in the dense layer than in the upper layer. Thus, the inclined part of the interface separates two regions of different ω. Viscosity smooths out this difference by means of an Ekman-type shear layer. In the weakly inclined part of the shear layer (say $r \approx 0.75$) the change of ω from one z-independent core to the other one occurs over a region with a dimensionless thickness of ≈ 0.06, in agreement with the expectation that the shear layer at the interface is of Ekman-type. This feature is also reflected by the behaviour of the streamlines, figure 7, which display recirculations below and above the inclined interface, of magnitude $E^{1/2}$.

In other words, the interfacial shear layer couples the spin-up processes of the lower and upper cores. This layer provides a two-way volume transport: from the centre to the periphery in the upper part, and in the opposite direction in the lower part. The faster rotating lower-core fluid viscously accelerates the light fluid in the upper part of the inclined shear layer and, thus, spins up the upper core. The upper fluid, on the other hand, has a decelerating effect on the the lower layer and, therefore, counteracts the spin up of the dense core.

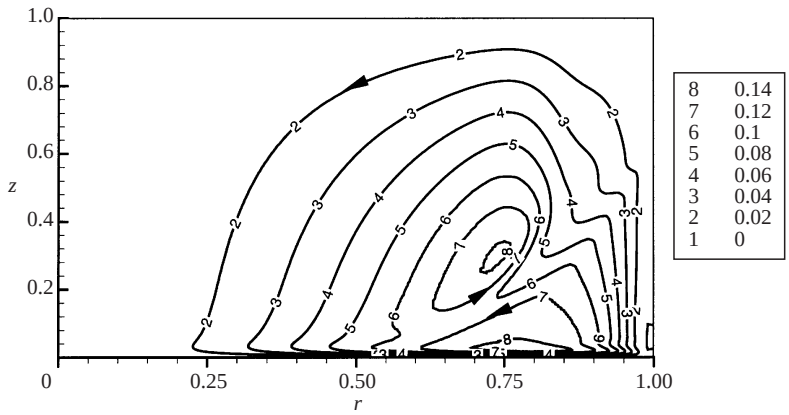

FIGURE 7. Stream-function contour lines $\psi/E^{1/2}$ corresponding to figure 5(*c*).

In the case presented, the stratification is weak ($Fr^2/9 > h_0$, see below), and hence a significant deformation of the interface occurs during the initial stages of the spin-up. During the first 10 revolutions the interface rises rapidly to about $3h_0$ at the periphery, and descends to almost $0.3h_0$ at small r. Eventually, the interface touches and intersects the bottom of the container (figure 5*c*, *d*). The circular region in which the upper-layer fluid is in direct contact with the bottom boundary is termed the bare spot. At this stage the upper-layer fluid is also directly affected by the strong Ekman layer friction at the bottom boundary and the spin-up of the lighter fluid becomes more effective. However, we notice that what is really important here is the area of the bare spot, not merely its presence; the spin-up of the upper layer can be significantly accelerated when the bare spot occupies a significant portion of the bottom boundary area.

The numerical results (figure 5*d*), moreover, indicate a possible mixing between the two fluids as the Ekman layer pumps upper-core fluid beneath the dense fluid. Such an intrusion was observed by Smeed (1987) in an experimental investigation of a related problem. Because of mixing and numerical diffusion, a clear-cut interface is indiscernible at larger times. Linden & van Heijst (1984) reported the tendency of the investigated flow to become unstable as time increases. In this case, the axial symmetry of the flow breaks down. Better numerical resolution at larger times would require costly computations on much finer grids, but a relation between the observed instability and the mixing predicted by the numerical code is anticipated. Therefore, the computations were not extended to larger times.

The secondary radial core velocity $u(r, z)$ scaled by $\sqrt{E}$ is displayed in figure 8. Again, in each layer u shows only a very weak axial dependence which carries over to large times. The oscillations at $t = 11$ rev, $z = 0.5$, 0.6, reflect the multiple shear-layer structure of the local flow field.

As expected for spin-up, the radial flow in the cores is negative. This allows transport of spun-up fluid from the periphery to the centre. The radial flow in the upper layer prior to the formation of the bare spot is driven by the interfacial shear layer and by the displacement of the interface. The value of u in the thick upper region is significantly smaller than in the thin lower layer which is directly affected by the bottom Ekman layer.

Figure 9 shows z-dependent profiles of the reduced pressure at different radial positions. (Note that the abscissa is directed from right to left.) This plot confirms

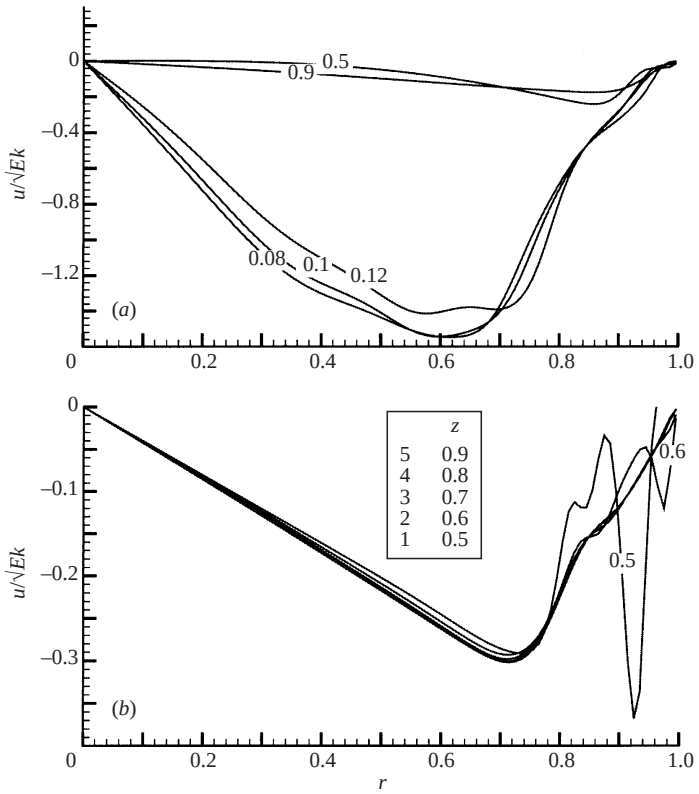

FIGURE 8. Radial velocity $u(r,z)/\sqrt{E}$ at successive t: (a) 4 rev, (b) 11 rev; $\epsilon = 5.1 \times 10^{-3}$, $Fr^2 = 8$, $E = 5 \times 10^{-5}$, $H = 1$, $h_0 = 0.2$.

that, as expected, the pressure distribution remains hydrostatic-cyclostrophic during the process. Although the flow is nonlinear (ω undergoes an $O(1)$ change during spin-up), the Ekman-layer-induced axial velocity is still too weak to support a substantial $\partial p/\partial z$ beyond the hydrostatic balance. Inside the upper layer, the reduced pressure is z-independent, and in the lower layer it varies linearly with z because of the additional body force term in the momentum balance for the lower layer, see (3.5)–(3.7). The slope discontinuity in the contour lines indicates the position of the interface.

4.2. *Asymptotical modelling*

The numerical results suggest that the fundamental behaviour of the flow field, for very small but realistic values of E, can be captured by a simplified model, an extension of Wedemeyer's (1964) homogeneous-fluid approximation for a two-domain system with a moving interface. The model is based on the combination of inviscid thick cores and asymptotically thin Ekman layers at the bottom and the interface. In each core the density is constant (1 and $1+\epsilon$) and the radial velocity, angular velocity and $\partial p/\partial r$ are z-independent. A similar approach was successfully employed by Lim *et al.* (1993) in an investigation of the spin-up from rest of a system of two thick layers of different fluids in a closed container. The details of the mathematical formulation are described in Appendix C.

Figure 10 illustrates the simplified flow field. Using the assumption of a hydrostatic-cyclostrophic pressure distribution, and the conditions of pressure continuity at the

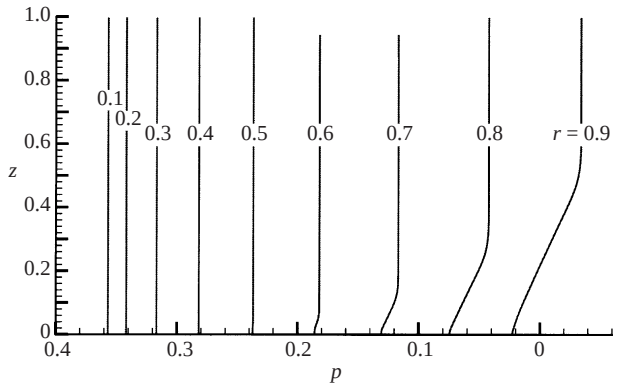

FIGURE 9. Reduced pressure p as a function of z for various r at $t = 11$ rev: $\epsilon = 5.1 \times 10^{-3}$, $Fr^2 = 8$, $E = 5 \times 10^{-5}$, $H = 1$, $h_0 = 0.2$.

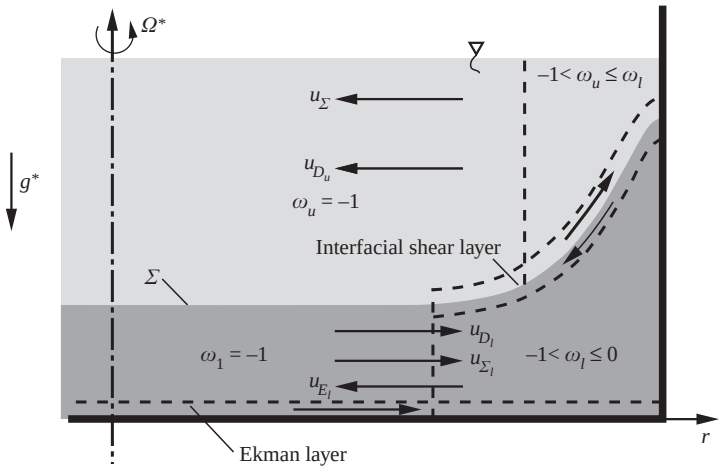

FIGURE 10. Schematic description of approximate flow-field model.

interface and of volume conservation for the lower layer, an equation for the height $h(r, t)$ of the interface in terms of the angular velocities in the cores is derived. It turns out that during the spin-up stage the local inclination of the interface, $\partial h/\partial r$, is essentially proportional to Fr^2 times the difference of the centrifugal accelerations in the lower and upper cores. Thus, the interface is horizontal where both layers of fluid are still non-rotating, and a strong inclination of the interface corresponds to the region where the lower fluid is already partly spun-up but the upper fluid is still not rotating. The spin-up fronts in the upper and lower cores are indicated by dashed vertical lines. The Ekman-type shear layers, which smooth out the differences of angular velocities between the different domains, are also marked by dashed lines.

Integral volume conservation requires that the radial volume fluxes in the shear layers at the bottom and at the interface are balanced by respective radial flows in the core. The Ekman layer induces an inwardly directed radial core component u_{E_l} in the dense region. The shear layer at the interface contributes u_{Σ_l} in the outward direction to the radial flow in the dense layer. The contribution of the interfacial shear layer to the radial core flow in the upper layer u_{Σ_u} is directed from the periphery to the

centre. Additional radial velocity components u_{D_l} and u_{D_u} are induced as a result of the axial motion (deformation) of the interface.

The azimuthal momentum balance in each core reflects the fact that the angular velocity increases in time due to convection of angular momentum (from the periphery to the centre), supplemented by a small radial shear term which smooths out the boundary conditions and the gradients of the spin-up front.

The mathematical manipulations of these balances lead finally to a coupled system for the variables h, ω_u and ω_u as functions of r and t which is significantly less complex than the original Navier–Stokes formulation. However, this model has several deficiencies which render it less useful than anticipated for practical simulations. First, the simple description fails when a bare spot appears, because the rim of such a region is a moving complex viscous 'corner' with merged Ekman layers. This restricts the use of the model to the short initial time periods or to configurations with small values of the parameter Fr^2 (see below). Second, we note that this approximation is asymptotical for $E \to 0$, but the accuracy is limited by some inherent errors. The flow field is strongly nonlinear (the Rossby number is not small) and the Ekman-layer transport formulas available for this case are merely integral correlations with typical errors of about 10%. Such errors are acceptable in our attempt to verify this model's ability to capture the essential features of the flow field. Third, no analytical solutions are in general available, in contrast to the homogeneous fluid case; however, some useful progress in this direction can be made, as follows.

4.2.1. *Analytical results*

Consider a special case in which the flow field in the lower core can be almost decoupled from flow field in the upper fluid. Indeed, for the initial stage of the spin-up process in the case when the deformations of the interface is weak (Fr^2 not large) and the upper layer is thick ($H/h_0 \gg 1$), we may expect the following approximate behaviour: spin-up is confined to the lower-layer region, while the fluid in the upper layer is unaffected. The lower-layer core is therefore subjected to the acceleration of the bottom Ekman layer and the hindrance of a free Ekman layer at the interface. The radial volume flux in the Ekman layer is approximated by the correlation

$$Q_b = \frac{E^{1/2}}{2} r(\omega_b - \omega_l), \tag{4.2}$$

where the subscript b denotes the horizontal boundary. In the present case, $\omega_b = 0$ for the bottom solid wall, and $\omega_b = 0.5(\omega_l - 1)$ on the interface Σ (i.e. the average value of the upper and lower cores). The radial velocity in the core is z-independent, and hence volume conservation dictates that the value of $-uh_0$ equals the sum of the Ekman fluxes on the top (interface) and bottom of the lower domain.

In the core of fluid of thickness h_0 outside the Ekman layers the inviscid balance of angular momentum is simply between the time-dependent and the radial advection terms. Under the previous considerations, this can be expressed as

$$\frac{\partial \Omega_l r^2}{\partial t} + \frac{E^{1/2}}{2h_0} \frac{1}{r} (-r^2 + \tfrac{3}{2}\Omega_l r^2) \frac{\partial \Omega_l r^2}{\partial r} = 0, \tag{4.3}$$

where

$$\Omega_l = \omega_l + 1, \tag{4.4}$$

and subject to the initial condition

$$\omega_l = -1 \quad (t = 0). \tag{4.5}$$

Equation (4.3) is, not surprisingly, of the form of Wedemeyer's inviscid equation (for a layer of fluid of height h_0), but in the present case the pumping effect of the upper layer is weaker than for a solid boundary, which leads to non-classical consequences.

The solution of (4.3) can be obtained by the method of characteristics. It reveals a moving spin-up front between stationary ($\omega_l = -1$) and partly spun-up fluid. We find that the representative spin-up time interval for the lower fluid is

$$\tau^*_{su-l} = 2\frac{h_0}{E^{1/2}\Omega^*}, \tag{4.6}$$

and that the spin-up front is at $r = \exp(-\mathscr{T})$, where $\mathscr{T} = t^*/\tau^*_{su-l}$. In the spun-up region the angular velocity is given by

$$\omega_l = \frac{2}{3}\frac{1 - \mathrm{e}^{-2\mathscr{T}}/r^2}{1 - \mathrm{e}^{-2\mathscr{T}}} - 1 \quad (\mathrm{e}^{-\mathscr{T}} \leqslant r < 1). \tag{4.7}$$

It is remarkable that in this case the lower core is not spun-up to solid-body rotation $\omega = 0$ during the local spin-up time interval, but rather attains a quasi-steady angular velocity $\omega_l = -1/3$. (A vertical shear layer, possibly of Stewartson type of thickness $\sim h_0^{1/2}E^{1/4}$, is needed near the wall $r = 1$ to reduce ω_l from $-1/3$ to zero, as detailed in Appendix C.) The value $\omega_l = -1/3$ reflects the balance between the driving friction of the solid bottom and the milder hindrance of the upper non-rotating fluid core.

During the relatively short time interval τ^*_{su-l} the friction torque of the bottom is reduced to $1/3$ of its initial value because of the spin-up of the lower fluid, and hence the subsequent increase of angular velocity of the system (recalling that the upper fluid is still at absolute rest) is expected to require a time period longer by a factor of about three than for a homogeneous fluid of height $H - h_0$, see (2.2).

The foregoing result allows a quick estimate of the maximal displacement of the interface from the initial position. Volume conservation and the pressure field, due to the hydrostatic–cyclostrophic balance and continuity at the interface, dictate that when $\omega_l = -1/3$ and $\omega_u = 0$ the height of the interface is, see (C 15),

$$h(r) = h_0 + \tfrac{1}{9}Fr^2(1 + \epsilon)(2r^2 - 1). \tag{4.8}$$

Formally, when $Fr^2(1 + \epsilon)/(9h_0) < 1$ then $h(r) > 0$ for $r \geqslant 0$ and a bare spot is not expected. In this case, the subsequent spin-up of the upper layer is caused mostly by the weak friction between the upper and the lower fluids. On the other hand, when $Fr^2(1 + \epsilon)/(9h_0) > 1$ we expect that the displacement of the interface plays an important role during the initial spin-up, including the formation of a bare spot; in this case the approximations (4.3)–(4.7) are not valid.

The foregoing analysis also indicates that the time required for the development of the conditions under which a bare spot can form is the spin-up time interval of the lower domain, given by (4.6). However, on account of the assumptions under which this result was derived, it can be used only as an estimate in the general case. For example, for the data employed in our computations in § 4.1 we obtain $\tau^*_{su-l} = 9$ rev, and figure 5 indicates the formation of the bare spot at about 11 rev.

In fact, the practical criteria for the appearance of the bare spot may be less clear-cut than the above-mentioned values of $Fr^2(1 + \epsilon)/(9h_0)$ and τ^*_{su-l} because of the non-rigorous considerations used in this derivation. Linden & van Heijst (1984) derived corresponding criteria for bare-spot formation in differential spin-up. They also assumed that the upper domain is thick and maintains its initial angular velocity, but postulated that the lower domain is fully spun-up, see Appendix C, § C.2. We think that the present approach, which takes into account the spin-up of the lower

layer subject to the hindrance friction from the upper domain, is more realistic. The friction from the upper core reduces the angular velocity in the lower core, and hence a larger threshold value of Fr^2 is required for the formation of the bare spot.

Linden & van Heijst (1984) estimated the time of formation of the bare spot by assuming that the interface descends with the initial axial suction velocity of the bottom Ekman layer. This yields, in the present case, half the value of the present τ^*_{su-l}. We think that this is an underestimate, because it does not account for the recirculation and the decay of the Ekman-layer suction with time, but may become relevant for very large values of Fr^2/h_0 when the behaviour of a homogeneous fluid is reproduced. The experiments of Linden & van Heijst (1984) show agreement, but with considerable scatter, with their estimate, and given the wide parameter range considered it not possible to extrapolate these observations to the present problem.

The validity of the model is checked and further information on the flow field obtained below, for a flow configuration with a smaller value of Fr^2 than used before in § 4.1.

4.3. *Case* $Fr^2 = 2$

In this case $\epsilon = 2.04 \times 10^{-2}$ and hence $g'^* = 20\,\mathrm{cm\,s^{-2}}$, four times larger than in the previous one, with other parameters unchanged. In figures 11–13, both full numerical and approximate-model results are displayed. Comparing figures 5 and 11, it is seen that the increase in stratification (a four times smaller Fr^2, but the same E and h_0) leads to a significant reduction of the interface deformation.

Figure 11 shows that there is good agreement between the approximate (dashed curve) and numerical predictions of the interface at $t = 4$ rev. At later times ($t = 8$ rev) the approximate results slightly underestimate h in a small region near the sidewall. However, for small radii the approximate curve is still very close to the position of the interface obtained from the Navier–Stokes numerical computations. (As time increases, some smearing of the $\phi(r, z)$-field around the interface appears, mostly in the non-rotating region, but this is a small effect when $\epsilon \ll 1$ as considered here, and outside the scope of our investigation.)

Figures 12 and 13 show comparisons between the approximate and numerical results for ω and $u/\sqrt{E}$ at $t = 2$ rev and $t = 8$ rev. The predictions of the approximate model for the velocity components of the lower layer ω_l and u_l are represented by dashed lines, and those of the upper layer ω_u and u_u are represented by dash-dotted lines. The approximate and numerical results for $\omega_{u,l}$ are in very good agreement. The agreement between the approximate and numerical results for the $O(E^{1/2})$ radial flow varies a little with time but is still fair. There should be no concern about the positive sign of u at $z = 0.4$ and $t = 2$ rev because the secondary flow is not yet fully developed in the upper layer at this early time.

Figure 14 shows the time evolutions of the angular velocities as predicted by the numerical solution of the two-layer system (solid curves, the value $z = 0.1$) and compared with analytical result (4.7) and (C 14) (dashed lines). It is seen that for a significant number of revolutions there is fair agreement between the results in the lower core region, regarding both the position of the spin-up front and the value of ω. The discrepancies can be attributed to the fact that in this case the displacement of the interface is not really small, and the spin-up front is smeared by viscous effects neglected by our analytical model. The agreement is expected to improve for smaller values of Fr^2/h_0 and E. Various tests, not detailed here, confirmed that, overall, the simple result (4.7) provides a useful approximation for the initial behaviour in the lower core when $Fr^2/9h_0 < 1$.

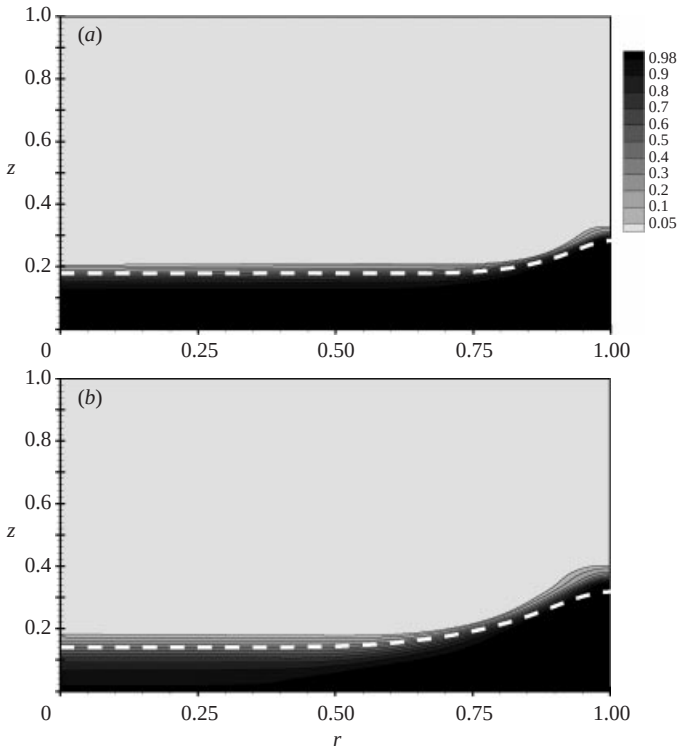

FIGURE 11. Numerical density function $\phi(r, z)$ contour plots and model predictions for the position of the interface (dashed line) at successive t: (a) 4 rev, (b) 8 rev; $\epsilon = 2.04 \times 10^{-2}$, $Fr^2 = 2$, $E = 5 \times 10^{-5}$, $H = 1$, $h_0 = 0.2$.

4.4. *Total angular momentum*

We have discussed the various details of the flow field during the Ekman-layer-dominated spin-up stage. The ultimate concern of the spin-up process is the behaviour of the total angular momentum in the container, $\Gamma(\tau)$, see (2.1). We now consider this global feature, as reflected in the previously discussed cases with $Fr^2 = 8$ and 2. For comparison, we add the homogeneous counterpart ($\epsilon = 0$ and $Fr \to \infty$).

The behaviour of $\Gamma(\tau)$ is presented in figure 15(a, b). In the first plot the numerically calculated $\Gamma(\tau)$ is scaled with the steady-state value corresponding to solid-body rotation. We observe that, as expected, Γ increases toward this value monotonically on the τ scale, and that the stratification hinders this process. Indeed, the fastest increase of Γ is for $Fr = \infty$ and the slowest for $Fr^2 = 2$. However, the influence of Fr^2 on $\Gamma(\tau)$ is not very dramatic. At $\tau = 0.4$ the value of Γ for $Fr = \infty$ is only 20% larger than for $Fr^2 = 2$.

Figure 15(b) displays the total angular momentum $\Gamma(\tau)$ obtained from numerical computations scaled with the value predicted by the Wedemeyer approximation based on the Ekman layers only, $\Gamma_{wed} = 0.25H(1 - \mathrm{e}^{-2\tau})$. We observe that the actual total angular momentum is larger than expected from the contribution of the Ekman layers, for all the tested values of Fr, at least for $\tau \leqslant 0.3$; the excess is about 40% at $\tau = 0.1$. Since the only additional source of angular momentum is the sidewall friction, we attribute to this source this excess of angular momentum.

Some further insight into the contribution of the sidewall friction to the growth of Γ can be obtained for the homogeneous-fluid case. The Ekman-layer dominance of

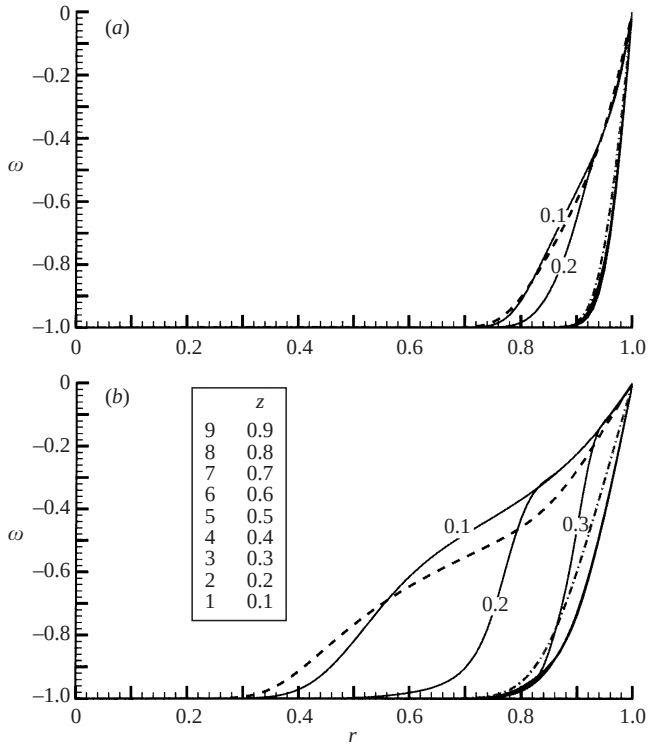

FIGURE 12. Numerical and approximate results for the angular velocity $\omega(r,z)$ at successive t: (*a*) 2 rev, (*b*) 8 rev; $\epsilon = 2.04 \times 10^{-2}$, $Fr^2 = 2$, $E = 5 \times 10^{-5}$, $H = 1$, $h_0 = 0.2$. The dashed and dot-dashed lines are predictions of the model for the lower and upper layers, respectively. Note that the numerical profiles mostly collapse onto a single line for each layer.

the spin-up process is an asymptotical $E \to 0$ result, and the leading term of $\omega(r,\tau)$ is given in table 1 in Appendix A. Let us use this ω to estimate the torque of the sidewall (per radian)

$$M_{sw} = HE\left(r\frac{\partial\omega}{\partial r}\right)_{r=1} = 2HE\frac{\mathrm{e}^{-2\tau}}{1-\mathrm{e}^{-2\tau}}, \tag{4.9}$$

while the Ekman layer torque is $M = 0.25E^{1/2}\mathrm{e}^{-2\tau}$, see (A 3). (Theses estimates must assume $\tau > E^{1/2}/H$, the formation time of the Ekman layers, of course.) The ratio between the Ekman-layer and the sidewall torques is $2HE^{1/2}/(1-\mathrm{e}^{-2\tau})$ and indicates that for small values of τ a significant contribution from the outer-wall torque is received. For the values of E and H in our case, and $\tau = 0.1$, the torque ratio is 0.32. We therefore expect that the value of Γ at $\tau = 0.1$ is at least 32% larger than evaluated by only the Ekman-layer friction result (A 3). This estimate is consistent with the numerical results of figure 15(*b*). Another test which we performed was the comparison of the numerically calculated torque of the bottom boundary with the Wedemeyer prediction (A 3); we found good agreement (the latter is actually slightly larger than the former).

5. Concluding remarks

The time-dependent flow field during the spin-up from rest about the vertical axis of a container with two fluids of different densities was analysed. Attention was

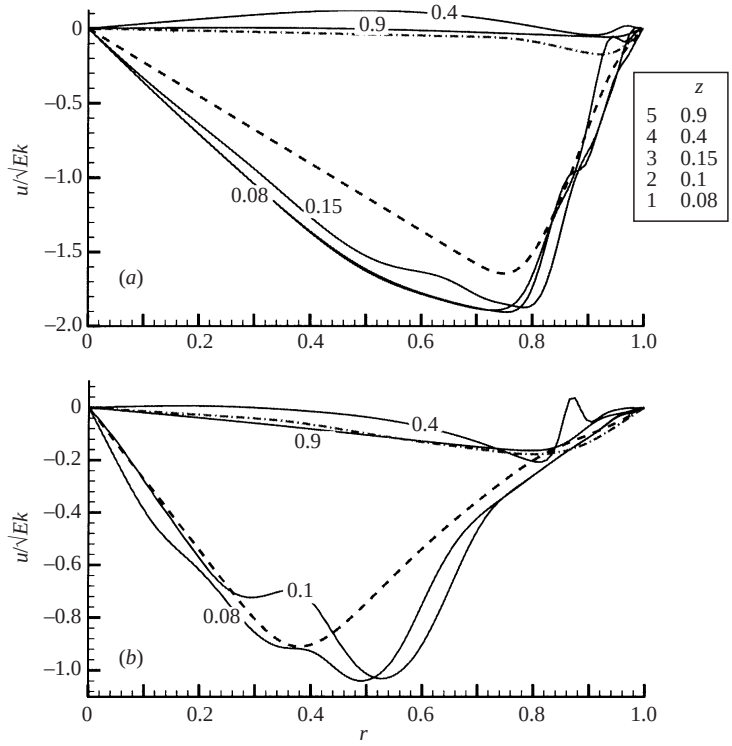

FIGURE 13. As figure 12 but for the radial velocity $u(r, z)/\sqrt{E}$.

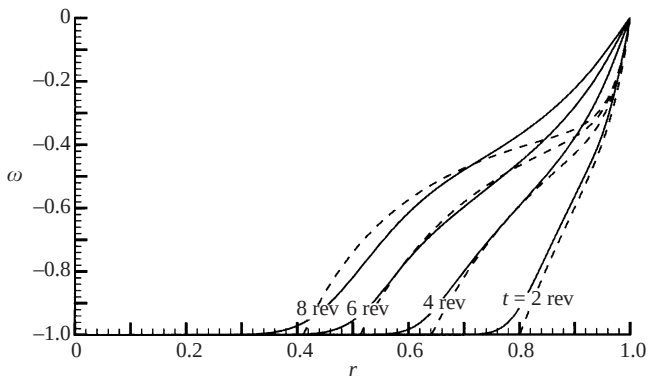

FIGURE 14. Numerical predictions (solid line) and predictions of the one-layer analytical model (dashed lines) at $z = 0.1$ for ω_l at successive t: $\epsilon = 2.04 \times 10^{-2}$, $Fr^2 = 2$, $E = 5 \times 10^{-5}$, $H = 1$, $h_0 = 0.2$.

focused on a configuration where the layer of lower fluid is thin, and the thicker upper layer has a free upper surface. Thus, the upper fluid is, for a part or all the spin-up time interval, not directly affected by the bottom Ekman layer friction and therefore the spin-up of this two-fluid system takes typically longer than in the homogeneous counterpart.

The numerical results presented, supported by asymptotical ($E \to 0$) approximate considerations, enhance our knowledge of the spin-up from rest process in this

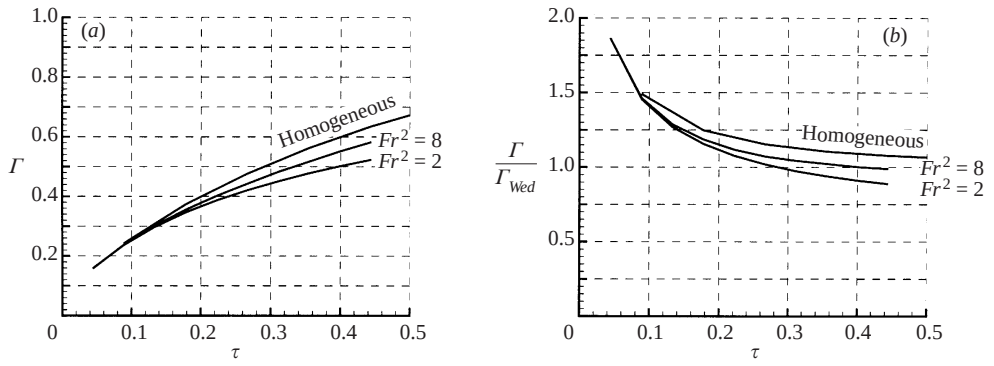

FIGURE 15. Total angular momentum as a function of τ. (*a*) Γ scaled with the steady-state value $0.25H$; (*b*) Γ scaled with the Wedemeyer-approximation-based value $0.25H(1-\mathrm{e}^{-2\tau})$.

more complex configuration, affected by a combination of centrifugal/Coriolis and (reduced) gravity accelerations. As in the homogeneous fluid case, the spin-up is driven mainly by the Ekman layer on the horizontal bottom boundary. The upper and lower fluids retain distinctive cores, with different z-independent angular velocities. The coupling between the cores is provided by an Ekman-like shear layer which develops on the deforming interface to smooth out the difference of ω. This shear layer drives the spin-up of the upper fluid layer and hinders the spin-up of the dense fluid in the lower layer. Typically, the dense fluid is spun up first, and subsequently acts as a partly spun-up buffer between the bottom and the thick upper layer.

The Ekman-layer dominance, z-independent radial and angular velocities in the cores and the fact that the pressure satisfies a hydrostatic–cyclostrophic balance motivated the formulation of a simple approximate model which facilitated the interpretation of the complex flow field under investigation.

When $Fr^2(1+\epsilon)/(9h_0) < 1$ and the lower core is much thinner than the upper core, the deformation of the interface is relatively small, and the fluid in the lower core is spun-up to about $2/3$ of the final value during a time $2h_0/(E^{1/2}\Omega^*)$ while the upper fluid remains essentially at rest. Next, the spin-up of the upper layer is driven by the weak Ekman layer on the interface. Since the friction at the bottom is reduced to $1/3$ of the initial value, the subsequent spin-up time interval for the upper fluid is expected to be prolonged by a factor 3 compared with a homogeneous fluid of the same thickness in direct contact with the boundary, see (2.2).

When $Fr^2(1+\epsilon)/(9h_0)$ is large the interface is strongly deformed during the spin-up process and a bare spot appears near the centre. At this spot the upper fluid makes contact with the bottom and this supplements the weak friction at the interface. The spin-up is more effective when a bare spot is present. However, what is important to the supply of angular momentum to the system is the size (radius) of this spot, not merely its presence, because the torque of a von Kármán layer over a disk of radius r is $\propto r^4$, see (2.2).

The previous considerations indicate that in a two-layer system the Ekman-layer spin-up interval is expected to be bounded by the relationship

$$1 < \tau^*_{su\ two\text{-}layer}/\tau^*_{su\ homogeneous} < 3 - 2h_0/H, \tag{5.1}$$

which reflects the transition from very large to very small values of Fr^2, i.e. from very weak to very strong stratification.

The density difference parameter, ϵ, assumed small, plays a passive role in the spin-up process. However, the maximal transient displacement of the interface during the spin-up may be $O(\epsilon^{-1})$ larger than at the end of the process.

The spin-up of a homogeneous fluid can be conceptually recovered as the limiting case of the two-fluid configuration in the asymptotic limit of $Fr \to \infty$ ($\epsilon \to 0$). As the density difference between the fluids is reduced – with angular velocity, geometry and viscosity of the systems fixed – the interface during spin-up becomes steeper and steeper until it coincides with the spin-up front in the aforementioned asymptotic limit.

The assumption of equal viscosities in both fluids can be easily relaxed. The expected qualitative consequences are an increased viscosity of the lower fluid enhancing the deformation of the interface and the appearance of the bare spot, and vice versa.

The ability of the relatively simple, fixed-grid numerical code, to reproduce the complicated flow field with a moving interface (which is both a kinematic shock and a detached shear layer) is remarkable, and gives credence to the use of this solver in other complex circumstances. An obvious extension is the investigation of the spin-up from rest of a three-layer fluid, which is underway and will be reported elsewhere. However, this numerical approach smears the kinematic shock (discontinuity of ϕ) over several grid intervals and consequently the value of ρ in this region may have errors of relative magnitude ϵ, see (3.1). This, in turn, may affect the local accuracy of the Ekman layer thickness, shear and transport results. To avoid this loss of accuracy the computations with this scheme must be restricted to small values of ϵ or to very fine grids. Solutions of this problem by different numerical schemes which provide high resolution of interfaces (e.g. volume of fluid) are worthy of consideration.

The main limitations of the present theoretical tools are (*a*) various numerical difficulties of stability and resolution which were encountered for large time intervals, and (*b*) the assumed axial symmetry. These deficiencies are plausibly connected with physical effects. Indeed, there are indications (Linden & van Heijst 1984) that baroclinic instabilities develop at the edge of the bare spot, and the numerical results indicate mixing in the interface domain after the spin-up of the lower fluid. These effects are inherently non-axisymmetric and cannot be reproduced by the present analysis. A combined experimental–theoretical approach is necessary to obtain more details of the flow field at more advanced times than considered here.

The present two-layer flow-field investigation provides useful insights into the continuously stratified fluid case, but the results cannot be carried over directly. The main differences between the two configurations are: (*a*) there is no clear-cut interface in a stratified fluid; (*b*) a strong z-dependence of u and ω is expected in the Ekman-layer-affected core of a stratified fluid. This problem needs a special analysis which is attempted in a separate study, see Flor, Ungarish & Bush (2002).

The authors would like to thank the Program of Scientific–Technological Cooperation Austria–Israel, the Christian Doppler Laboratory for Continuous Solidification Processes, and the Fund for the Promotion of Research at the Technion University, Israel, for their financial support of this project.

Appendix A. Homogeneous fluid approximation

Wedemeyer (1964) suggested the use of a momentum-integral correlation between the angular velocity jump and the volume transport in the Ekman-type layer. Simi-

	$0 \leqslant r^2 \leqslant \mathrm{e}^{-2\tau}$	$\mathrm{e}^{-2\tau} \leqslant r^2 \leqslant 1$
$2HE^{-1/2}u$	$-r$	$\mathrm{e}^{-2\tau}(r-1/r)/(1-\mathrm{e}^{-2\tau})$
$\omega+1$	0	$(1-\mathrm{e}^{-2\tau}/r^2)/(1-\mathrm{e}^{-2\tau})$
$wE^{-1/2}$	$z/H-1$	$-\mathrm{e}^{-2\tau}(z/H-1)/(1-\mathrm{e}^{-2\tau})$

TABLE 1. Velocity field for spin-up from rest of a homogeneous fluid with open boundary at $z = H$ and solid bottom at $z = 0$ (see figure 2) according to Wedemeyer (1964). Here $\tau = t^*/\tau^*_{su}$ and $\tau^*_{su} = 2H/(E^{1/2}\Omega^*)$.

larity with the linear (small differential rotation) case gives the simple form

$$Q = -0.5E^{1/2}r[\omega(z = 0^+) - \omega_{bottom}], \tag{A 1}$$

where Q is the radial volume flux (per radian) carried by the shear layer and 0^+ denotes the core of fluid. In the spin-up from rest problem $\omega_{bottom} = 0$. The velocity field in the inviscid interior is expanded in a power series of $E^{1/2}$, and the leading terms, subject to the governing equations and volume transport matching with (A 1), yield the results given in table 1.

The total angular momentum is

$$\Gamma(t) = \int_0^H \int_0^1 [\omega(r, z, t) + 1]r^3 \,\mathrm{d}r \,\mathrm{d}z = 0.25H(1 - \mathrm{e}^{-2\tau}), \tag{A 2}$$

and the torque imposed by the Ekman layer on the fluid in these circumstances (per radian) is

$$M = 0.25E^{1/2}\mathrm{e}^{-2\tau}. \tag{A 3}$$

We note in passing that various attempts have been made to modify and improve this model, but the simple results used here capture well the qualitative and quantitative behaviour of the problem under investigation, see Weidman (1976*a*, *b*) and Duck & Foster (2001), where other pertinent references are also given. (The simplest correction is a quantitative one, suggested by the solution of von Kármán's rotating disk problem: to introduce a multiplication factor 0.89 in the right-hand side of (A 1), which also means that $E^{1/2}$ should be multiplied by this factor in the subsequent results. But in practical cases this correction is of the order of magnitude of the neglected terms in the approximation, and hence not really important.)

Appendix B. The finite-difference code

B.1. *Time discretization*

Consider the time advance of a flow field variable denoted by f at time t to the new value denoted by f^+ at time $t + \delta t$. A forward-in-time finite-difference technique is used. One time step for the momentum equation (3.5) with the Coriolis and pressure terms treated implicitly and other terms treated explicitly yields

$$\boldsymbol{v}^+ + 2\delta t\hat{\boldsymbol{z}} \times \boldsymbol{v}^+ = -\frac{\delta t}{1 + \epsilon\phi}\nabla p^+ + \delta t\boldsymbol{X} + \boldsymbol{v} \equiv \boldsymbol{B}, \tag{B 1}$$

where

$$\boldsymbol{X} = -\boldsymbol{v} \cdot \nabla\boldsymbol{v} + \frac{1}{1 + \epsilon\phi}[\boldsymbol{f}\phi + E\nabla^2\boldsymbol{v}]. \tag{B 2}$$

By means of simple vector algebra manipulations (as discussed in detail by Ungarish 1993, p. 303) an explicit expression for $\boldsymbol{v}^+$ is obtained from (B 1):

$$\boldsymbol{v}^+ = \frac{1}{1+4\delta t^2}[\boldsymbol{B} + 4\delta t^2(\hat{\boldsymbol{z}}\cdot\boldsymbol{B})\hat{\boldsymbol{z}} - 2\delta t\hat{\boldsymbol{z}}\times\boldsymbol{B}]. \tag{B 3}$$

Next the divergence operator is applied to both sides of this expression and the continuity equation (3.4) is imposed on $\boldsymbol{v}^+$. The result is an elliptic equation for the pressure p^+ at $t+\delta t$,

$$\nabla\cdot\frac{1}{1+\epsilon\phi}\nabla p^+ + 4\delta t^2\frac{\partial}{\partial z}\frac{1}{1+\epsilon\phi}\frac{\partial p^+}{\partial z} - \nabla\cdot\boldsymbol{X} - 4\delta t^2\frac{\partial}{\partial z}\hat{\boldsymbol{z}}\cdot\boldsymbol{X} \\ -2\delta t\hat{\boldsymbol{z}}\cdot\nabla\times\boldsymbol{X} - 4\delta t\frac{\partial w}{\partial z} - 2\hat{\boldsymbol{z}}\cdot\nabla\times\boldsymbol{v} - \frac{\nabla\cdot\boldsymbol{v}}{\delta t} = 0. \tag{B 4}$$

Theoretically, the last term is zero, but for preventing an accumulation of numerical errors it is sometimes useful to keep it in the calculations. Substitution of the boundary conditions (3.13)–(3.15) for $\boldsymbol{v}$ into the appropriate components of (B 1) yields Neumann-type boundary conditions $\partial p^+/\partial r$ and $\partial p^+/\partial z$ for (B 4). They define p^+ up to an arbitrary constant. The pressure $p_{il,1}$ is set to 0 for definiteness. Using the solution for p^+, the velocity field $\boldsymbol{v}^+$ is straightforwardly obtained from (B 3).

The ϕ^+ field is calculated next using the scalar equation (3.8). In principle, this completes the time step advance, and a new cycle can be attempted.

B.2. *Spatial discretization*

The numerical, staggered grid is sketched in figure 3. The method of central differences was employed for all terms except for the advection terms in the ϕ transport equation (3.8). The discontinuity of ϕ may introduce spurious numerical oscillations in the solution of (3.8). To reduce this effect, for this equation, according to MacCormack's explicit method, the following predictor–corrector stages were used for each time step:

$$\left.\begin{aligned} \phi^p_{i,j} &= \phi_{ij} - \delta t(Adv_f\phi)_{i,j} + \delta t(Dif\phi)_{ij}, \\ \phi^c_{i,j} &= \phi^p_{ij} - \delta t(Adv_b\phi^p)_{ij} + \delta t(Dif\phi^p)_{i,j}, \\ \phi^+ &= 0.5(\phi_{ij} + \phi^c_{ij}), \end{aligned}\right\} \tag{B 5}$$

where Adv_f and Adv_b denote the advection terms as approximated by forward and backward differencing. Dif denotes the diffusion terms approximated by central differences, as illustrated by (3.21).

The axial stretching function used is

$$z = H(a^{\mathscr{Z}} - 1)/(a^H - 1), \tag{B 6}$$

where the constant $a > 1$ is prescribed. Both the physical grid z and the uniform grid $\mathscr{Z}$ are in the range $[0, H]$, $\mathscr{Z}_j = (j-0.5)\delta\mathscr{Z}$ and $\delta\mathscr{Z} = H/jl$ for $j = 1(1)jl$. For example, for $H = 1$ and $jl = 200$ we used $a = 2.5$ to obtain the first interval, at the bottom, as $z_{3/2} = 3.0613\times10^{-3}$, while the Ekman layer thickness $3E^{1/2} = 21.2\times10^{-3}$. Stretching for the detached Ekman layer was not attempted, because it would require a dynamic-adjustable grid. Moreover, the thickness of the detached layer is larger by a factor of at least 2 than that at the bottom, and hence our grids provided good resolution of this layer without special stretching.

Appendix C. Mathematical formulation of the approximate model

It is assumed that $\sqrt{E} \ll 1$ and that the flow during the period of time considered here is governed by the secondary circulation of the thin quasi-steady Ekman-type layers at the bottom plate and the interface Σ. The arguments of Wedemeyer's (1964) homogeneous-fluid spin-up theory (see also Greenspan 1968 and Ungarish 1993) indicate the following orders of magnitude for the flow variables in the inviscid core: $\omega = v/r \sim 1$; $u, w \sim E^{1/2}$. In the present case we distinguish between the variables in the upper and lower cores using the subscripts u and l. In each core the radial and angular velocities, u and ω, are expected to be z-independent and the axial velocity w to vary linearly with z. The cores are separated by the interface $z = h(r,t)$. Let us introduce the *absolute* angular velocities in the cores

$$\Omega_{u,l}(r,t) = v_{u,l}(r,t)/r + 1. \tag{C 1}$$

The pressure field in each core satisfies the hydrostatic–cyclostrophic balance taking account of the appropriate density, and the pressure is continuous on the interface. These considerations yield, after some algebra, a connection between the position of the interface and the angular velocities

$$h(r,t) = h_W(t) - Fr^2 \left[\int_r^1 (\Omega_l^2 - \Omega_u^2)\bar{r}\,\mathrm{d}\bar{r} + \epsilon \int_r^1 \Omega_l^2 \bar{r}\,\mathrm{d}\bar{r} \right], \tag{C 2}$$

where $h_W(t)$ denotes the value at the sidewall $r = 1$. This is readily obtained from the volume conservation requirement of the lower-layer fluid (assumed to start at $r = 0$),

$$h_W(t) = h_0 + Fr^2 \left[\int_0^1 (\Omega_l^2 - \Omega_u^2) r^3\,\mathrm{d}r + \epsilon \int_0^1 \Omega_l^2 r^3\,\mathrm{d}r \right]. \tag{C 3}$$

We note that the largest displacements of the interface are contributed by the first integral in the last two equations, because the second integral is multiplied by the small ϵ. However, this contribution can be significant only during the early stages of spin-up, when the angular velocity difference between the upper and lower cores is of order unity.

The azimuthal momentum equation can be written to leading order as

$$\frac{\partial v_{u,l}}{\partial t} + u_{u,l}\left(\frac{1}{r}\frac{\partial}{\partial r}(r v_{u,l}) + 2\right) = E\left[\frac{\partial^2 v_{u,l}}{\partial r^2} + \frac{\partial}{\partial r}\left(\frac{v_{u,l}}{r}\right)\right]. \tag{C 4}$$

The initial and boundary conditions are

$$v = -r \quad (t = 0 : 0 \leqslant r \leqslant 1) \quad \text{and} \quad v = 0 \quad (t \geqslant 0^+ : r = 0, 1). \tag{C 5}$$

In order to solve (C 4) directly, a simple expression for the radial velocities $u_{u,l}$ in terms of the azimuthal velocities $v_{u,l}$ is needed. At the bottom of the container, a thin Ekman layer develops in about one third of a revolution. Because the adjustment time of the Ekman layer is much shorter than the spin-up timescale, the Ekman layer can be considered quasi-steady. During spin-up, the flow inside the asymptotically thin Ekman layer (thickness $O(E^{1/2})$) is from the centre to the periphery. Following Wedemeyer (1964), integral volume conservation yields

$$u_{E_l} = \frac{E^{1/2}}{2}\frac{1}{h} v_l < 0 \tag{C 6}$$

for the contribution of the Ekman-layer volume transport to the radial lower-layer core flow. The difference in angular velocities between the partly spun-up region in

the lower layer and the upper layer causes the formation of a Ekman-type shear layer at the interface. This inclined shear layer supports the spin-up of the upper layer and hinders the spin-up of the lower layer. Its contributions to the core flows in the respective layers are incorporated as

$$u_{\Sigma_l} = \frac{\beta}{1+\beta}\frac{1}{2}\left(\frac{E}{\cos\alpha}\right)^{1/2}\frac{1}{h}(v_l - v_u) > 0, \tag{C 7}$$

$$u_{\Sigma_u} = \frac{1}{1+\beta}\frac{1}{2}\left(\frac{E}{\cos\alpha}\right)^{1/2}\frac{1}{H-h}(v_u - v_l) < 0, \tag{C 8}$$

where α denotes the local angle of inclination of the interface and $\beta = (\rho_u^*/\rho_l^*)\sqrt{\nu_u^*/\nu_l^*}$. We note that the foregoing Ekman-layer contributions are based on a linear analysis (i.e. small perturbations around solid-body rotation), but in the present problem the nonlinear effects are not small. This places an inherent limitation on the accuracy of the model.

In addition to the contributions of the shear layers, the radial flows $u_{D_{u,l}}$ induced by the axial deformation of the interface must also be considered. Conservation of volume yields

$$u_{D_l} = -\frac{1}{rh}\int_0^r \frac{\partial h}{\partial t}\bar{r}\,\mathrm{d}\bar{r}, \tag{C 9}$$

$$u_{D_u} = \frac{1}{r(H-h)}\int_0^r \frac{\partial h}{\partial t}\bar{r}\,\mathrm{d}\bar{r}. \tag{C 10}$$

The derivative $\partial h/\partial t$ can be obtained either directly by a backward-difference approximation or iteratively. The values of u_l and u_u are the sums of the contributions (C6)–(C10), which closes (C4). Equation (C 4) was solved by an explicit FTCS finite-difference discretization subject to a CFL condition. A MacCormack and a Crank–Nicholson discretization were also tested and led to similar results. In test runs the code successfully reproduced the parabolic shape of the free surface of a single fluid in solid-body rotation and the analytical result for the spin-up from rest of a pure fluid as given in table 1.

C.1. *Small-Fr^2 case*

Assume that the stratification is strong and the upper layer much thicker than the lower layer of fluid. In this case the additional approximation $h = h_0$ and $v_u = -r$ can be made in the previous equations, and the solution of (C 4)–(C 7) is of interest only in the lower layer. For $\alpha = 0$ (horizontal interface) and $\beta = 1$ (fluids of similar viscosities and densities) we obtain

$$u_l = \frac{1}{4}E^{1/2}\frac{1}{h_0}(3v_l + r). \tag{C 11}$$

We substitute this result into (C 4). The inviscid ($E = 0$) form of this equation yields (4.3), and therefore the solution in the interior of the lower region is

$$\omega_l = \frac{2}{3}\frac{1 - \mathrm{e}^{-2\mathscr{T}}/r^2}{1 - \mathrm{e}^{-2\mathscr{T}}} - 1 \quad (\mathrm{e}^{-\mathscr{T}} \leqslant r < 1) \tag{C 12}$$

and $\omega_l = -1$ for $r < \mathrm{e}^{-\mathscr{T}}$, where $\mathscr{T}$ is the time scaled with $\tau^*_{su-l} = 2h_0/(E^{1/2}\Omega^*)$.

However, we observe that $\omega_l(r = 1) = -1/3$ and hence a shear layer is needed to satisfy the boundary condition $\omega_l(r = 1) = 0$. We denote by $\tilde{\omega}$ the angular velocity

in this region. The balance in this layer is provided by the steady-state viscous form of (C 4). In linearized simplified form, this is a classical Coriolis–shear balance of Stewartson-layer type which reads

$$2u_l = E\frac{\mathrm{d}^2\tilde{\omega}}{\mathrm{d}x^2}, \tag{C 13}$$

where $x = 1 - r$, and u_l is given above (but simplified by the fact that now $r \approx 1$). The result, subject to the boundary conditions, is

$$\tilde{\omega} = -\frac{1}{3}\left(1 - \exp\left[-\sqrt{\frac{3}{2h_0}}E^{-1/4}x\right]\right). \tag{C 14}$$

C.2. *Constant Ω_u and Ω_l approximation*

When both Ω_u and Ω_l are constants (or functions of t only) equations (C 2)–(C 3) can be combined and easily integrated to yield the explicit result

$$h(r,t) = h_0 - \tfrac{1}{4}Fr^2\Omega_l^2\left[1 - \left(\frac{\Omega_u}{\Omega_l}\right)^2 + \epsilon\right](1 - 2r^2). \tag{C 15}$$

Linden & van Heijst (1984) developed a similar result for differential spin-up from angular velocity $1 - \Delta$ to 1 (in our notation), where $0 < \Delta < 1$. They used the assumption that the lower layer is fully spun up ($\Omega_l = 1$ in our notation) and the upper layer rotates with the initial angular velocity, $1 - \Delta$; moreover, they neglected the typically very small ϵ in (C 15). In this case,

$$h(r,t) = h_0 - \tfrac{1}{4}Fr^2[1 - (1 - \Delta)^2](1 - 2r^2). \tag{C 16}$$

According to this estimate, a bare spot (i.e. $h \leqslant 0$) is expected when (a) $Fr^2/(4h_0) > 1$ and (b)

$$\Delta \geqslant 1 - \left(1 - \frac{4h_0}{Fr^2}\right)^{1/2}, \tag{C 17}$$

which is, upon proper re-scaling, similar to (4.5) in that paper.

However, the present analysis indicated that the Ekman layer on the interface between the upper and lower cores prevents full spin-up of the lower region unless a similar state is attained in the upper region. A more realistic estimate is that, while $\Omega_u = 1 - \Delta$, the lower core can attain only $\Omega_l = 1 - \Delta/3$. If these values are used in (C 15), slightly different, and perhaps more accurate, forms of (C 16) and (C 17) are obtained. In general, larger threshold values of Fr and Δ than those predicted by (C 16) and (C 17) are obtained.

REFERENCES

Amberg, G. & Ungarish, M. 1993 Spin-up from rest of a mixture: numerical simulation and asymptotic theory. *J. Fluid Mech.* **246**, 443–464.

Berman, A. S., Bradford, J. & Lundgren, T. S. 1978 Two-fluid spin-up in a centrifuge. *J. Fluid Mech.* **84**, 411–431.

Duck, P. W. & Foster, M. R. 2001 Spin-up of homogeneous and stratified fluids. *Annu. Rev. Fluid Mech.* **33**, 231–263.

Flor, J. B., Ungarish, M. & Bush, J. W. M. 2002 Spin-up from rest in a stratified fluid: boundary flow. *J. Fluid Mech.* **472**, 51–82.

Goller, H. & Ranov, T. 1968 Unsteady rotating flow in a cylinder with a free surface. *Trans. ASME: J. Basic Engng* **90**, 445–454.

Greenspan, H. P. 1968 *The Theory of Rotating Fluids*. Cambridge University Press.

Greenspan, H. P. & Howard, L. N. 1963 On time-dependent motion of a rotating fluid. *J. Fluid Mech.* **17**, 385–404.

Hallworth, M. A., Huppert, H. E. & Ungarish, M. 2001 Axisymmetric gravity currents in a rotating system: experimental and numerical investigations. *J. Fluid Mech.* **447**, 1–29.

Hyun, J. M., Leslie, F., Fowlis W. W. & Warn-Varnas, A. 1983 Numerical solutions for spin-up from rest in a cylinder. *J. Fluid Mech.* **127**, 263–281.

Kim, K. Y. & Hyun, J. M. 1994 Spin-up from rest of a two-layer liquid in a cylinder. *Trans. ASME: J. Fluids Engng* **116**, 808–814.

Lambert, C. F., Linden, P. F., Lowenthal, D. & Stern, M. E. 1983 Benthic fronts and the global excess radon distribution. *Geophys. Astrophys. Fluid Dyn.* **25**, 309–315.

Lim, T. G., Choi, S. & Hyun, J. M. 1993 Transient interface shape of a two-layer liquid in an abruptly rotating cylinder. *Trans. ASME: J. Fluids Engng* **115**, 324–329.

Linden, P. F. & van Heijst, G. J. F. 1984 Two-layer spin-up and frontogenesis. *J. Fluid Mech.* **143**, 69–94.

Pedlosky, J. 1967 The spin-up of a stratified fluid. *J. Fluid Mech.* **28**, 463–479.

Press, W. H., Teukolsky, S. A., Vetterling, W. T. & Flannery, B. P. 1992 *Numerical Recipes in Fortran*. Cambridge University Press.

Smeed, D. A. 1987 A laboratory model of benthic fronts. *Deep-Sea Res.* **34**, 1431–1459.

Ungarish, M. 1993 *Hydrodynamics of Suspensions*. Springer.

Weidman, P. 1976*a* On the spin-up and spin-down of a rotating fluid. Part 1. Extending the Wedemeyer model. *J. Fluid Mech.* **77**, 685–708.

Weidman, P. 1976*b* On the spin-up and spin-down of a rotating fluid. Part 2. Measurements and stability. *J. Fluid Mech.* **77**, 709–735.

Wedemeyer, E. H. 1964 The unsteady flow within a spinning cylinder. *J. Fluid Mech.* **20**, 383–399.